Developmental Biology 451 (2019) 158–166

Contents lists available at ScienceDirect

Developmental Biology

journal homepage: www.elsevier.com/locate/developmentalbiology

Original research article

FGF10 is an essential regulator of tracheal submucosal gland morphogenesis

Alison J. May [a,1], Tathyane H.N. Teshima [a,b], Alistair Noble [c], Abigail S. Tucker [a,*]

[a] Centre for Craniofacial and Regenerative Biology, Guy's Hospital, King's College London, United Kingdom
[b] Department of Stomatology, School of Dentistry, University of Sao Paulo, Brazil
[c] MRC & Asthma UK Centre in Allergic Mechanisms of Asthma, King's College London, United Kingdom

ARTICLE INFO

Keywords:
Branching morphogenesis
Development
Airway
Fibroblast growth factor
Respiratory disease

ABSTRACT

Mucus secretion and mucociliary clearance are crucial processes required to maintain pulmonary homeostasis. In the trachea and nasal passages, mucus is secreted by submucosal glands (SMGs) that line the airway, with an additional contribution from goblet cells of the surface airway epithelium. The SMG mucus is rich in mucins and antimicrobial enzymes. Defective tracheal SMGs contribute to hyper-secretory respiratory diseases, such as cystic fibrosis, asthma, and chronic obstructive pulmonary disease, however little is known about the signals that regulate their morphogenesis and patterning. Here, we show that *Fgf10* is essential for the normal development of murine tracheal SMGs, with gland development arresting at the early bud stage in the absence of FGF10 signalling. As *Fgf10* knockout mice are lethal at birth, inducible knockdown of *Fgf10* at late embryonic stages was used to follow postnatal gland formation, confirming the essential role of FGF10 in SMG development. In heterozygous *Fgf10* mice the tracheal glands formed but with altered morphology and restricted distribution. The reduction in SMG branching in *Fgf10* heterozygous mice was not rescued with time and resulted in a reduction in overall tracheal mucus secretion. *Fgf10* is therefore a key signal in SMG development, influencing both the number of glands and extent of branching morphogenesis, and is likely, therefore, to play a role in aspects of SMG-dependent respiratory health.

1. Introduction

Airway mucus secretion plays a critical role in the muco-ciliary clearance of billions of airborne particles and pathogens daily. Respiratory mucus is produced by the goblet cells of the surface epithelium and the submucosal glands (SMGs) found within the submucosal layer of the nasal, tracheal and bronchial cavities (Sturgess and Imrie, 1982; Borthwick et al., 1999; May and Tucker, 2015). The structure of tracheobronchial SMGs are characterised into three domains: (1) the distal secretory gland, (2) the medial collecting duct and (3) the proximal ciliated duct (*reviewed in* May and Tucker, 2015). The distal region consists of two distinct secretory cell types, responsible for producing airway mucus. Serous cells produce a solution primarily consisting of mucin MUC7, proteoglycans and bactericidal proteins such as lactoferrin and lysozyme (Masson et al., 1966; Klockars and Reitamo, 1975; Finkbeiner, 1999), while mucous cells produce a gel rich in MUC2 and MUC5b and antimicrobial peptide cathelicidin (Buisine et al., 1999; Finkbeiner, 1999). Collectively these secretions provide a barrier to the exposed surface airway epithelium. While the cellular composition of SMGs is homologous across mammals, SMG distribution can change between species. In mice, respiratory SMGs are found within the walls of the nasal cavity and extend to the upper trachea, with most tracheal SMGs found between the cricoid cartilage and the first tracheal cartilage ring. SMGs in mice only extend to the seventh cartilage ring, however in humans glands extend more caudally throughout the trachea and bronchi (Borthwick et al., 1999; Sturgess and Imrie, 1982).

The need to understand the morphogenesis, structure and function of the SMGs is emphasised by the role they play in respiratory diseases such as cystic fibrosis (CF), asthma and chronic obstructive pulmonary disease (COPD). Abnormal mucus secretion from tracheal and nasal SMGs is characteristic of patients with CF (Joo et al., 2010; Salinas et al., 2005; Jeong et al., 2015), contributing to decreased mucociliary clearance of the airways and onset of pulmonary infection. Further evidence in the pig model of CF shows that mucus hypo-secretion (Joo et al., 2010; Cho et al., 2011), and increased mucus tethering from the SMGs (Hoegger et al., 2014) give rise to hindered muco-ciliary clearance, prior to the onset of

* Corresponding author.
E-mail address: abigail.tucker@kcl.ac.uk (A.S. Tucker).
[1] Current address: Program in Craniofacial Biology, Department of Cell and Tissue Biology, University of California, 513 Parnassus Avenue, San Francisco, CA, 94143, USA.

https://doi.org/10.1016/j.ydbio.2019.03.017
Received 8 January 2019; Received in revised form 26 March 2019; Accepted 26 March 2019
Available online 6 April 2019

inflammation, indicative that SMG morphology and function are primary defects of CF pathogenesis. Mouse models of CF have been shown to have abnormal distribution of tracheal SMGs, with an increase in proximal numbers of SMGs in diseased animals (Borthwick et al., 1999). Moreover, early onset of hypertrophy in SMGs is characteristic of infants with CF (Oppenheimer and Esterly, 1975; Sturgess and Imrie, 1982). Chronic asthma sufferers also show signs of SMG secretory cell hyperplasia (Aikawa et al., 1992; Rogers, 2004), while sufferers of COPD show mucous cell hyperplasia that gives rise to mucus-hypersecretion and airway plugging (Reid, 1960; Rogers, 2008).

Development of SMGs undergoes typical patterns common to other branching organs such as the lung, salivary gland and mammary gland (Tucker, 2007; Hannezo et al., 2017). Tracheal SMG morphogenesis can be described in four stages (Keswani et al., 2011; Thurlbeck et al., 1961). Stage 1 of development defines the specification and emergence of an initial gland bud from the respiratory epithelium (Fig. 1, A). Stage 2 is characterised by elongation of the epithelial bud into the underlying mesenchyme, and the onset of cavitation within the stalk as lumen formation begins (Fig. 1, A). Stage 3 describes the continual clefting and branching of the SMG, alongside lumen formation. Stage 4 is classified by cellular differentiation, indicated by mucus production within the distal glandular secretory cells (Fig. 1, A).

A few studies have shed light on the signalling pathways involved in tracheal SMG development and patterning. *Eda/Edaradd* expression is required for early gland initiation and budding as tracheal SMG number is severely reduced in both the *Tabby* (*Eda* mutant), and *Crinkled* mice (*Edaradd* mutant) at postnatal day 7 (Rawlins and Hogan, 2005). Furthermore, human patients with hypohidrotic ectodermal dysplasia, caused by defects in the EDA pathway, have reduced numbers of respiratory SMGs, asthma-like symptoms, and respiratory tract infections (Callea et al., 2013). *Wnt/β-catenin* activation of lymphoid enhancer factor *Lef-1* is also required for early SMG bud specification and outgrowth (Xie et al., 2014). The transcription factor Sox2 inhibits expression of *Lef-1,* while WNT signalling reduces *Sox2* expression in the SMG placode. Therefore, WNT signalling leads to reduced Sox2 and an increase of *Lef-1* transcripts in SMG placodes, suggesting a dynamic relationship between WNT signalling and *Sox2* expression during SMG bud specification (Xie et al., 2014).

In vertebrates, fibroblast growth factors (FGFs) make up one of the largest family of polypeptide proteins with 22 ligands (FGF1-FGF22) and four cell membrane-bound FGF receptors (FGFRs) (Ornitz and Itoh, 2001). *Fgf10/Fgfr2b* signalling is required for successful development of many branched organs (Ohuchi et al., 2000). Lung morphogenesis is inhibited in the absence of *Fgf10* and *Fgfr2b* expression, and *Fgf10* and *Fgfr2b* homozygous mice die at birth due to lung agenesis (Sekine et al., 1999; Min et al., 1998; De Moerlooze et al., 2000). Morphogenesis of the submandibular salivary gland is arrested at the initial bud stage at embryonic day E12.5 in both *Fgf10* and *Fgfr2b* homozygous (−/−) mice, and salivary glands are hypoplastic and secrete a reduced volume of saliva in *Fgf10* heterozygous (+/−) adults (May et al., 2015). More recently it has been shown that *Fgf10* maintains *Sox9* expression and regulates Sox9+ epithelial progenitor cell expansion during salivary gland morphogenesis (Chatzeli et al., 2017).

The tracheal SMGs have not been investigated in the complete absence of Fgf10 signalling, however *Fgf10* heterozygous mice have a reduction in the number of SMGs at postnatal day 20 compared to wildtype littermates (Rawlins and Hogan, 2005). The glands present in the tracheal submucosa had undergone less branching and were restricted to the anterior trachea, with no glands found between the more posterior cartilaginous rings (Rawlins and Hogan, 2005). Considering this altered phenotype, we investigated the role of FGF10 in early tracheal SMG development using both knockout and conditional

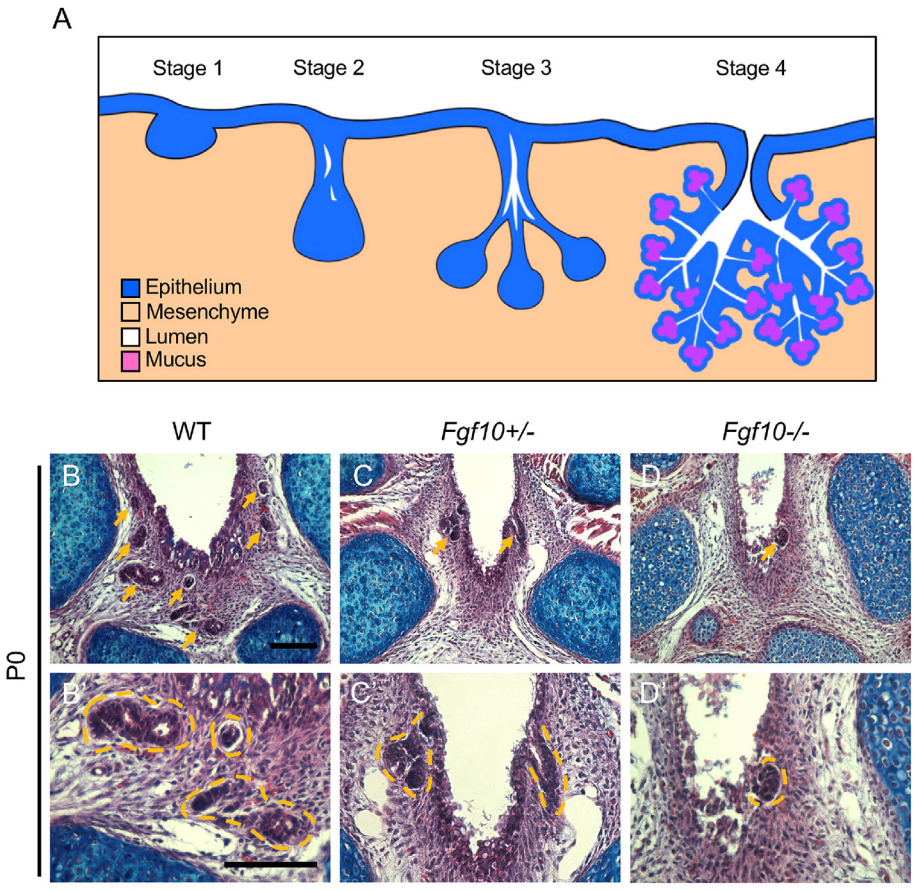

Fig. 1. *Fgf10* is essential for successful tracheal gland branching morphogenesis. **(A)** Schematic representation of the four stages of tracheal gland branching morphogenesis. Stage 1: Tracheal SMG buds first invaginate from the respiratory epithelium into the underlying mesenchyme. Stage 2: Elongation of the bud occurs, and cavitation begins lumen formation. Stage 3: Epithelial stalk undergoes clefting and branching and lumen formation continues. Stage 4: Continual branching and cellular differentiation occurs indicated by mucus production by acinar cells. (B–D) Frontal trichrome stained images of the anterior trachea at postnatal stage (P) 0. (B′-D′) High power images of B-D. (B,B′) WT SMGs reached lumen formation and branching stages in the ventral trachea at P0. (C. C′) *Fgf10* +/- SMGs form lumens, however branching of the glands was reduced. (D, D′) Gland buds were found in *Fgf10* −/− mice however they had not elongated from the respiratory epithelium. Scale bar in B, B' = 100 μm, same scale in other images. Arrows indicate SMGs, orange outline SMGs in higher magnification images. Cartilages stain blue with alcian blue.

knockout mice.

2. Materials and methods

2.1. Experimental animals

Fgf10-deficient mice were first generated by Min et al. (1998) (Mouse Genome Informatics ID 1099809). Investigation was carried out on WT (n = 3), *Fgf10* +/− (n = 2) and *Fgf10* −/− (n = 4) for P0 SMG analysis and WT (n = 7) and *Fgf10* +/− (n = 6) for adult SMG analysis. For inducible ablation experiments, the ubiquitous *pCAGGCre-ERT2* allele (Hayashi & McMahon, 2002) was crossed to *Fgf10 floxed* (Fgf10A02 tmc1c) mice on a C57BL/6 background (produced by MRC-Harwell as part of the International Mouse Phenotyping Consortium (IMPC; Skarnes et al., 2011; Bradley et al., 2012)). *Fgf10*fl/fl females were crossed to *pCAGCre-ERT2/+;Fgf10*fl/+ males to generate *pCAGCre-ERT2+/+; Fgf10*fl/fl (WT;$Fgf10^{fl/fl}$, n = 3), *pCAGCr-eERT2/+;Fgf10*fl/+ (Cre^{ERT2}; $Fgf10^{fl/+}$, n = 3) and *pCAGCre-ERT2/+;Fgf10*fl/fl (Cre^{ERT2};$Fgf10^{fl/fl}$, n = 3) mouse pups, which were collected at postnatal day (P)21. *R26-tdTomato* reporter line (Gt(ROSA)26 Sor tm14(CAG-tdTomato)Hze JAX labs) was used to confirm the activity of the *Cre* induced by tamoxifen and were mated to *Fgf10*fl/fl males to generate *Fgf10*fl/fl;*R26RtdTom* females. These were mated to *PCAGcreERT2/+;Fgf10*fl/+ males and the Tomato was observed with a Nikon SMZ25 fluorescence microscope. Fgf10/lacZ/+ reporter mice carrying a nuclear-targeted lacZ insertion that does not disrupt Fgf10's coding exons, were mated and postnatal pups were provided by Mohammad Hajihosseini (n = 3) (Kelly et al., 2001; Hajihosseini, 2008). All procedures and culling methods were performed under a project license approved by the United Kingdom's Home Office and in accordance with the Animal (Scientific Procedures) Act of 1986, United Kingdom.

2.2. Animal collection

Mice were mated in the late evening. Midday of the day at which a vaginal plug was discovered was recorded as embryonic day (E) 0.5. Adult males and females were culled by exposure to rising levels of CO_2 gas or by cervical dislocation. Primers used to detect wildtype *Fgf10* locus were 5′-GAGGAAATGCTGCGCACAATGTATACTCGG-3' (Fgf203 forward primer) and 5′-GGATACTGACACATTGTGCCTCAGCCTTTC-3' (Fgf204 reverse primer), while the mutant *Fgf10* locus was detected by primers 5′-GCTTGGGTGGAGAGGCTATTC-3' (Fgf233 forward primer) and 5′-CAAGGTGAGATGACAGGAGATC-3' (Fgf234 reverse primer) of the neocassette insert (Sekine et al., 1999). The inducible loss of *Fgf10* was performed by administering 75 mg of tamoxifen/kg body weight intraperitoneally in corn oil into E17.5 pregnant mice, and 15 μg/g into each pup at postnatal day 2. Corn oil injections alone has been shown to lead to no activation of this *Cre* line (Hayashi and McMahon, 2002). E17.5 was chosen as this is 24 h prior to the induction of SMG in the trachea (May and Tucker, 2015). Tamoxifen recombination time was expected to occur 24 h after administration (Danielian et al., 1998). Tamoxifen was injected in combination with progesterone to counter the negative effects of tamoxifen on the ability to give birth naturally (Lizen et al., 2015). At this dose of tamoxifen the recombination of this *Cre* line is not 100% penetrant (Hayashi and McMahon, 2002). Therefore a second injection was given postnatally at P2. Mice were then culled at postnatal day 21.

2.3. Histological staining

Upon collection, trachea were fixed in 4% paraformaldehyde in PBS (PFA) overnight at 4 °C. Tissue was dehydrated in increasing methanol concentrations and left overnight at 4 °C in Isopropanol (Sigma Aldrich). Samples were cleared in 1,2,3,4 Tetrahydronaphthalene at RT, and embedded in paraffin wax. Alternative serial 8 μm sagittal sections were collected along the dorsal/ventral axis of each trachea. Paraffin embedded sections were dewaxed using Histoclear and rehydrated through an ethanol series. Tracheal sections were stained using a Trichrome stain of 1% Alcian Blue, Ehrlich's Haematoxylin and 0.5% Sirius Red in saturated Picric Acid.

2.4. X-gal staining of Fgf10 LacZ+/− postnatal submucosal glands

Trachea of postnatal day 7 (P7) were fixed in PFA 4% overnight at 4 °C, followed by two washes in 2 μM of magnesium chloride ($MgCl_2$) in PBS for 5 and 15 min at RT. Samples were then washed in a solution of 0.1% of Deoxycholic Acid, 0.2% of Igepal NP-40, 1 μM of $MgCl_2$ in PBS for 5 min at RT. Staining was performed using the previous solution with 5 mM of $K_3Fe(CN)_6$, 5 mM of $K_4Fe(CN)_6$ and 1mg/mL of X-gal in Dimethyl sulfoxide (DMSO) overnight at 37 °C. Samples were washed in PBS and post-fixed in PFA overnight at 4 °C to stop the reaction, followed by the paraffin embedding process. Sections of 8-10 μm were then counterstained in 0.5% of alcoholic eosin and mounted with Neomount (Merck Millipore).

2.5. Cartilaginous staining of embryonic tracheal tissue

Trachea were dissected from E18.5 *Fgf10* WT and *Fgf10* +/- littermates and fixed overnight in 95% ethanol in deionised H_2O at 4 °C. After 24 h of fixation, fat from the tissue was removed by storing the trachea in 100% acetone overnight at RT. Followed by two rinses in 95% ethanol, trachea were placed in Alcian Blue solution (15 mg Alcian Blue 8GX in 80 ml 95% ethanol and 20 ml glacial acetic acid) for 24 h rocking at RT. Tissue was rinsed with 95% ethanol twice for 30 min and stored in 95% ethanol overnight at RT. Trachea were cleared in 1% Potassium Hydroxide (KOH) for 3–4 h. Tissue went through a series of 1% KOH and glycerol solutions, at RT. Tissue was stored in 100% glycerol imaged using a Leica MZFLiii dissection microscope fitted with a Leica DFC300 Fx camera.

2.6. Mucus secretion analysis

Mice aged 7–8 weeks (WT; n = 4, *Fgf10* +/−; n = 6) were culled by exposure to rising levels of CO_2 and trachea were immediately dissected. The thyroid gland and oesophagus were removed, and the trachea was cut along the dorsal trachealis muscle (Supplementary Fig. 1, A). The following procedure was modified from the method used by Ianowski et al. (2007). Using insect pins, the trachea was opened and pinned to a sylgard plate and the luminal mucosal surface was exposed (Supplementary Fig. 1, B). The mucosal side of each trachea was dried with air spray and 5 μl of mineral oil (Sigma) was added to the surface. Beneath the trachea, 2.5 μl of D-MEM/F12 plus penicillin/streptomycin and 1% Glutamax (Invitrogen) medium was added to nourish the tissue during incubation (Supplementary Fig. 1, B). Tracheal tissue was placed in a 5% CO_2 incubator at 37 °C for 10 min. The exposed trachea was placed under a Leica MZFLiii dissection microscope fitted with a Leica DFC300 Fx digital camera. A further 2.5 μl of DMEM/F12 medium containing 60 μM of the cholinergic carbachol (Sigma) was added to the medium bath, giving a final concentration of 30 μM carbachol, leading to stimulation of the tracheal glands. Photographs of the anterior region of the trachea were taken every 30 s for 10 min to trace mucus bubble production.

After 10 min of exposure to carbachol, the total number of mucus bubbles produced were counted. Viable bubbles for area measurement were those which followed the criteria described in Ianowski et al. (2007): (a) a complete circular outline surrounding each mucus bubble so that accurate measurements could be collected and (b) no fusion with adjacent droplets. For gland opening analysis these criteria were not followed, as they were not required to count the amount of bubbles produced. The area of each bubble was calculated in micrometres (μm^3) ImageJ software. Overall trachea mucus secretion was calculated by the sum of all areas of each bubble per animal. Statistics and graphs were calculated using Microsoft Excel and Graphpad Prism software.

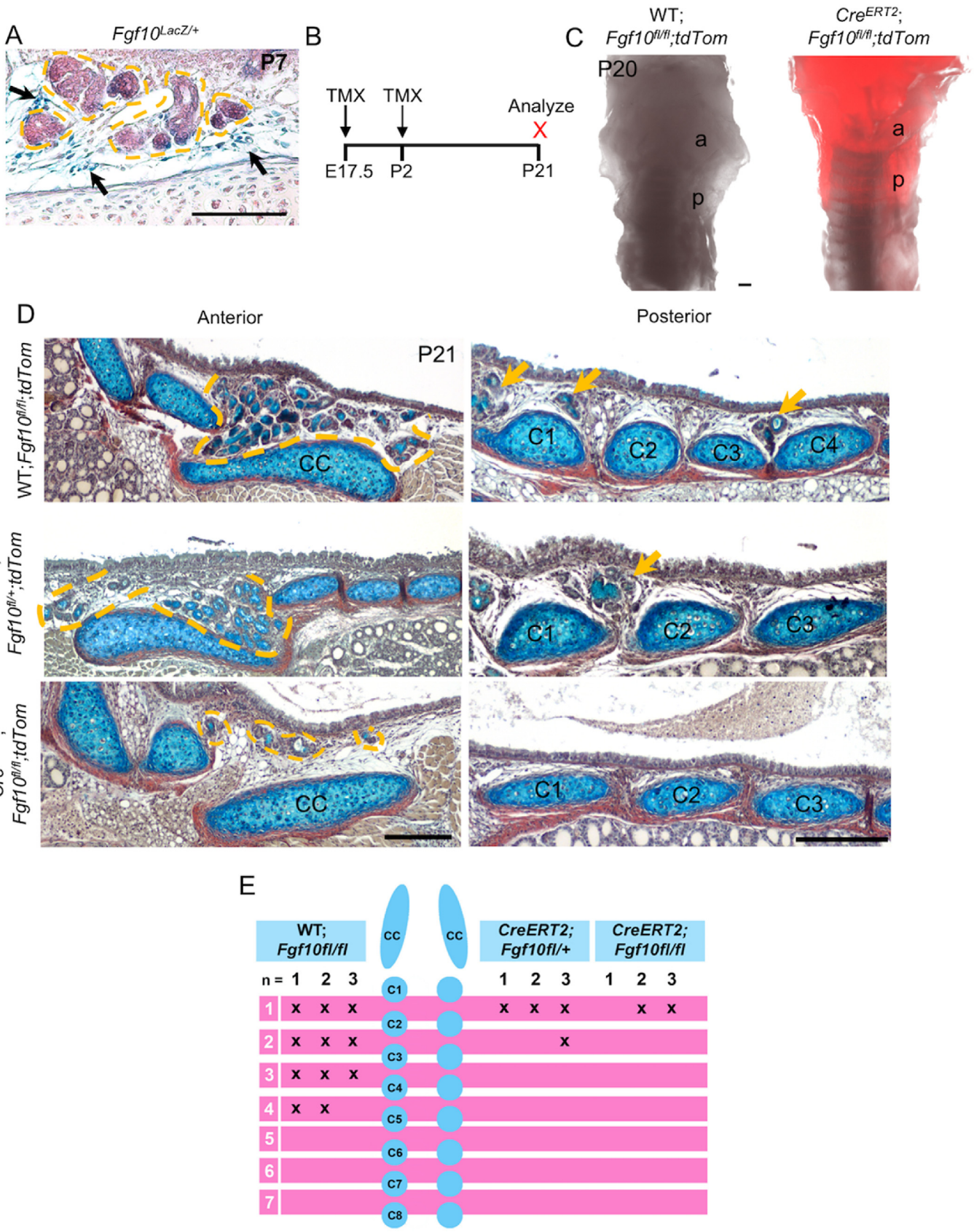

(caption on next page)

Fig. 2. Tracheal SMG morphogenesis is inhibited after conditional ablation of *Fgf10* during postnatal SMG development. **(A)** *Fgf10*$^{LacZ/+}$ trachea at postnatal day (P) 7 stained with X-gal (blue – arrows) to show *Fgf10* expression surrounding SMGs. **(B)** Time-course of tamoxifen (TMX) administration of wildtype (WT) and *Cre*^{ERT2};*Fgf10*$^{fl/fl}$; *tdTom* mice. TMX was given to pregnant females at embryonic day (E)17.5 and individual pups on P2. Trachea were analysed on P21. **(C)** Confirmation of inducible *Cre* recombination in the anterior (a) and posterior (p) trachea by the expression of R26tdTomato (red). **(D)** A significant loss in anterior SMG branching is evident in P21 *Fgf10* conditional knock-out mice adjacent to the cricoid cartilage (CC), with a reduction in SMG branch expansion into the mesenchyme compared to WT. Heterozygous mice showed a slight reduction in anterior SMG branching. **(D, E)** Posterior SMGs are present between the cartilage rings (C1-C4) in WT animals at P21, however are reduced in heterozygous and homozygous *Fgf10* mutant mice. (E) Schematic of gland distribution. N numbers represent each specimen analysed while pink bars represent mesenchymal space where SMGs are found between each cartilage ring (C1-8). X indicates presence of SMGs at P21. Scale bar in A = 100 μm, C & D = 200 μm. Orange outline indicates anterior SMGs. Arrows indicate posterior SMGs.

3. Results

3.1. Complete loss of Fgf10 leads to defective tracheal SMG development

To investigate the role of *Fgf10* during early stages of tracheal SMG development, glands were analysed in *Fgf10* +/- and *Fgf10* −/− mice. Although *Fgf10* −/− mice die at birth due to lung agenesis (Min et al., 1998; Sekine et al., 1999), initiation of SMGs can be analysed as anterior glands start to emerge from the tracheal epithelium at Embryonic day (E) 18.5 (May and Tucker, 2015). *Fgf10* mutant pups were collected on E19/P (postnatal day) 0 as the mother was giving birth. In wildtype (WT) animals, anterior glands had budded, elongated, cavitated and commenced branching (Fig. 1, B, B′). Similar stages of development were observed in heterozygous (*Fgf10* +/−) littermates however gland development appeared delayed and branching of the formed glands reduced (Fig. 1, C, C′). In the complete absence of *Fgf10* in homozygous animals (*Fgf10* −/−), some gland buds were found emerging from the surface epithelium, however development was arrested at this bud initiation stage with no glands found at a distance from the tracheal surface (Fig. 1, D. D′). This indicates that the SMGs did not undergo later stages of branching morphogenesis and that *Fgf10* expression is not required for initial epithelial gland bud specification but is required for subsequent successful bud elongation and branching.

3.2. Time inducible loss of Fgf10 during postnatal development reduces anterior tracheal SMG branching and posterior SMG expansion

To further investigate the role of *Fgf10* during SMG morphogenesis, we turned to later stages of postnatal gland development. First, we analysed *Fgf10* expression in *Fgf10*$^{LacZ/+}$ mice at P7. Xgal staining revealed *Fgf10* expression in the mesenchyme surrounding the developing SMG (Fig. 2, A). To follow development of the tracheal SMGs at postnatal stages we moved to a time inducible *Fgf10* knockout mice (*Cre*^{ERT2};*Fgf10*$^{fl/fl}$;*tdTom*). Tamoxifen was administered to pregnant females at E17.5, just as the most anterior tracheal SMGs were starting to initiate, and again to individual pups at P2, with tracheal tissue collected at P21 (Fig. 2, B). As *Fgf10* −/− mice die at birth, due to agenesis of the lungs (Sekine et al., 1999; Min et al., 1998), ablation of FGF10 using the inducible knockout mouse allowed pups to develop to E17.5 with adequate Fgf10 expression, but permitted our continued study of SMG development in the absence of Fgf10 from E18.5. Earlier injection was not attempted due to potential compromised development of the palate, which is reliant on *Fgf10* expression (Rice et al., 2004; Teshima et al., 2016). Tamoxifen inducible *Cre* recombination was confirmed in the anterior and posterior trachea by the expression of R26tdTomato (red – Fig. 2, C). No Tomato was observed in control Cre negative *Fgf10*$^{fl/fl}$;tdTom pups (Fig. 2, C). Trichrome staining of tracheal sections concluded a significant loss of anterior SMG branching adjacent to the cricoid cartilage in *Cre*^{ERT2};*Fgf10*$^{fl/fl}$ animals compared to control Cre negative littermates (Fig. 2 D, orange outline). A slight reduction in anterior SMG branching was observed in heterozygous *Cre*^{ERT2};*Fgf10*$^{fl/+}$ littermates (Fig. 2, D). Additionally, an absence of SMGs located posterior to the cricoid cartilage, in between the tracheal cartilage rings was evident in both *Cre*^{ERT2};*Fgf10*$^{fl/+}$ and *Cre*^{ERT2};*Fgf10*$^{fl/fl}$ animals, while in control mice SMGs reached the 4th cartilage ring (C4) (Fig. 2D and E). These results further support the necessity of *Fgf10* in tracheal SMG elongation and branching.

3.3. Anterior and posterior tracheal SMGs are reduced in Fgf10+/- adult mice

It has previously been reported that there is an altered SMG phenotype in adult *Fgf10* +/- mice, with a reduction in branching of the anterior SMGs adjacent to the cricoid cartilage and a severe reduction in the posterior expansion of the glands between each tracheal cartilage ring in adult *Fgf10* +/− (Rawlins and Hogan, 2005). We investigated adult WT and *Fgf10* +/- littermates and observed a similar phenotype in our mouse line with a reduction in anterior tracheal SMGs in heterozygous animals compared to their WT littermates (Fig. 3, A). Variation in severity of this reduction was observed in *Fgf10*+/- mice, however the number of glands was always decreased in the heterozygous adults compared to WT littermates (Fig. 3A and B). Analysis of SMGs between tracheal cartilage rings also showed a notable reduction in the anterior-posterior presence of the glands (Fig. 3, B). The majority of adult WT littermates showed continuous SMG development between each cartilage ring, most often reaching the mesenchyme between the 6th and 7th ring (Fig. 3, B). Posterior initiation therefore continues between P21 and 6 weeks in WTs. In *Fgf10* +/- mice, posterior expansion of the SMGs was significantly reduced, with small SMGs only found above the 3rd cartilage ring. In a previous study investigating tracheal SMG formation in the *Tabby* mouse, which has deficient *Eda* signalling, the pseudostratified epithelium of the trachea showed a disorganized appearance and increased height of columnar epithelial cells compared to WT animals (Rawlins and Hogan, 2005). In our study, no epithelial abnormalities were observed in the *Fgf10* +/- animals compared to their WT littermates (Fig. 3, C).

Fgf10 has been shown to be expressed in the ventral tracheal mesenchyme from E12.5-E16.5 when tracheal patterning is underway (Sala et al., 2011). Additionally, *Fgf10* null embryos have truncated trachea with disorganized rings (Sala et al., 2011). As SMGs form between the tracheal cartilage rings, we wanted to ensure that the observed altered SMG phenotype in *Fgf10* +/- animals was not a secondary defect due to abnormal cartilage patterning. This hypothesis was ruled out using whole mount Alcian Blue staining, however, as no difference in cartilage phenotype between WT and *Fgf10* +/- littermates was observed (Supplementary Fig. 1, A).

3.4. Fgf10 +/− adult mice showed reduced tracheal SMG openings and overall mucus secretion

Using histological methods, it was difficult to conclude whether the heterozygous mice showed a reduction in branching of each gland, a reduction in the number of glands within the anterior mesenchyme, or collectively both of these mechanisms. We therefore moved to a live tracheal explant model to follow mucous production. Previous papers have used the application of mineral oil to the mucosal tracheal surface to investigate SMG fluid secretion (Joo et al., 2001; Ianowski et al., 2007). We therefore used this model to assess whether the defect in branching led to a reduction in the amount of mucus secreted into the airway lumen in heterozygous animals compared to their WT littermates (Supplementary Fig. 1B and C). A time line of images was taken of the tracheal tissue in culture during mucus production stimulated by carbachol over a

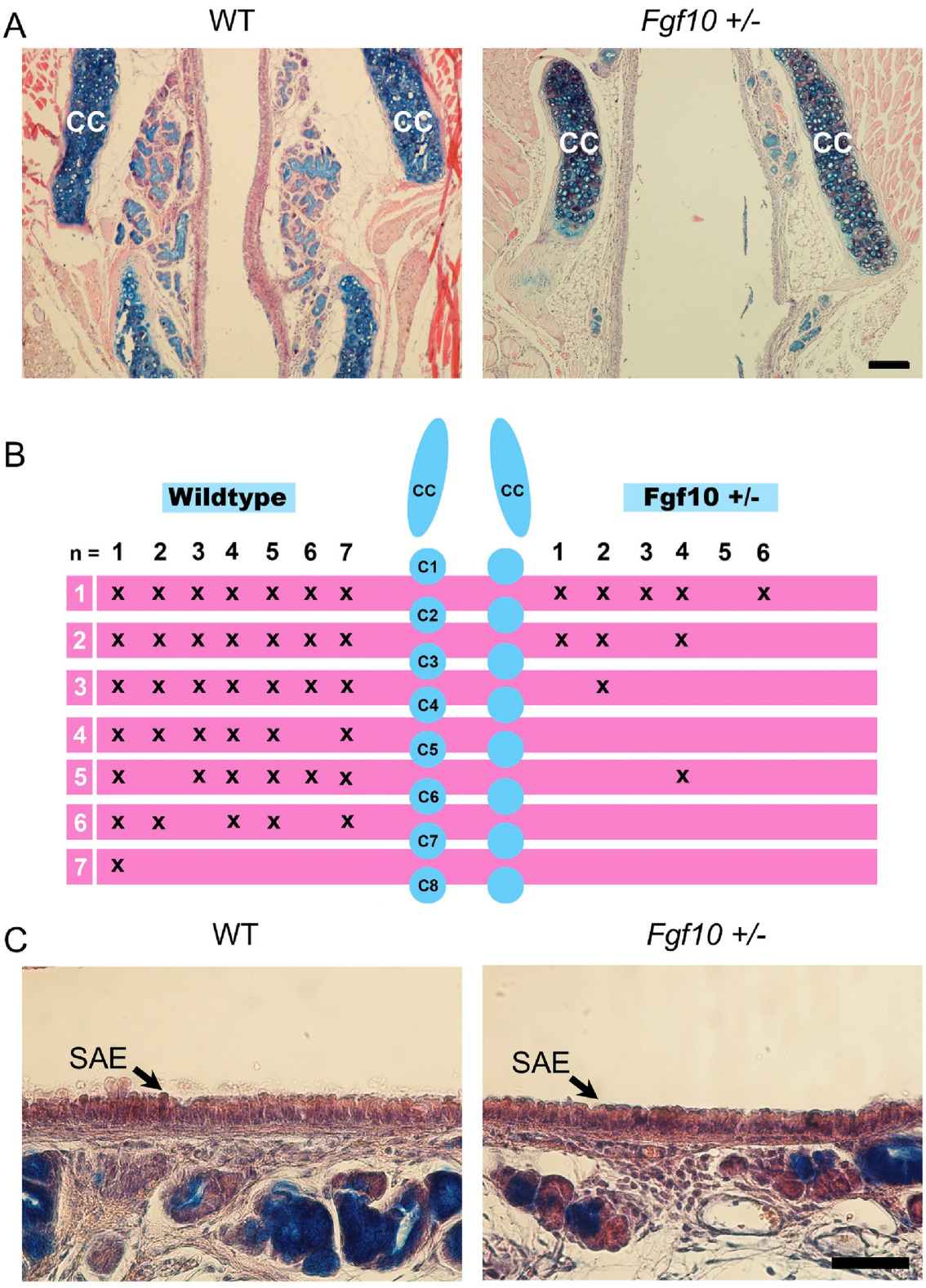

Fig. 3. *Fgf10* +/− tracheal SMG phenotype is not recovered in adult animals. **(A,C)** Frontal sections through adult tracheas stained with trichrome. **(A)** WT adults show extensively branched anterior SMGs adjacent to the cricoid cartilage (CC) while *Fgf10* +/- littermates show a significant reduction in glands in a similar plane. Scale bar = 100 μm. **(B)** Posterior extension of the SMGs is noticeably reduced in *Fgf10* +/− animals compared to their WT littermates. N numbers represent each specimen analysed while pink bars represent mesenchymal space where SMGs are found between each cartilage ring (C1-C8). X indicates presence of SMG. **(C)** No obvious differences were observed in the tracheal epithelium of adult WT and *Fgf10* +/− littermates at 6–10 weeks. Scale bar in A, C = 50 μm.

10-min period. Images were analysed and the number of mucus bubbles present between the cricoid cartilage (CC) and Tracheal cartilage 2 (C2) were counted. Each bubble represented the presence of a gland opening. Results elucidated that the number of bubbles was significantly reduced in *Fgf10* +/- animals ($p < 0.001$), indicating a decrease in the number of functional glands within the mesenchyme of the trachea between the anterior cartilage rings in *Fgf10* +/- adults (Fig. 4A and B). While analysis of the area of each individual bubble did not differ significantly between the two groups ($p = 0.429$), the overall amount of mucus secreted (sum of all bubble areas) was significantly reduced in *Fgf10* +/- adults (Fig. 4, B, $p < 0.001$). Together with the histological analysis of *Fgf10* heterozygous adult mice, these results indicate a reduction in total mucus secreted within the tracheal lumen compared to WT littermates.

4. Discussion

The present study takes a number of approaches to show that Fgf10 signalling is essential for the development of tracheal submucosal glands. Our results conclude that although SMG bud initiation may be *Fgf10* independent, the later stages of gland branching, cellular differentiation and gland secretion are significantly compromised in the absence of *Fgf10* expression.

As anterior tracheal SMGs in the ventral part of the tube start initiating at E18.5 in our mouse line, this gave us an opportunity to collect *Fgf10* −/− pups at P0, along with their WT and *Fgf10* +/- littermates, to investigate the effect of loss of Fgf10 on gland initiation. Interestingly, gland buds were found in ventral and slightly more dorsal anterior positions in the *Fgf10* −/− specimens collected. This result showed that *Fgf10* is not required for the initiation of the epithelial gland primordia or development of the initial gland bud, however it is essential for glands to progress to later development. The role of Fgf10 in these later morphogenetic stages was further supported by a reduction in SMG branching observed in *Fgf10* +/- pups at P0. Ventral glands of WT animals had reached the lumen formation stage and were undergoing clefting and branching while *Fgf10* +/- littermates displayed glands that had elongated into the underlying mesenchyme and formed lumens but showed evident reduced branching. This phenotype mirrors that reported for both the submandibular salivary gland (Jaskoll et al., 2005; Wells et al., 2013; Teshima et al., 2016; Chatzeli et al., 2017) and mammary gland (Mailleux et al., 2002) in *Fgf10* −/− mice, where gland development does not progress passed the bud stage and branching is reduced leading to aplastic glands. This suggests that Fgf10 signalling in particular is not needed for gland initiation, a conserved role reported in a variety of glandular organs, but is essential for subsequent development stages and that other ligands are essential for initial gland budding. One such factor may be Fgf7, which also signals through Fgfr2b. *Ex vivo* studies of the developing submandibular salivary gland have shown that Fgf7, through activated MEK and PI3K signalling cascades, is required for salivary gland budding, and that Fgf10 promotes branching and elongation of gland ducts through MEK 1/2 signalling (Steinberg et al., 2005). Furthermore, both recombinant Fgf7 and Fgf10 induce ectopic bud formation of the lacrimal gland epithelium in mouse embryonic ocular cultures (Makarenkova et al., 2000). This suggests that Fgf7 may promote SMG initial bud formation, or compensation in the absence of Fgf10 signalling to induce SMG bud outgrowth. Furthermore, we have previously shown that *Fgf10* expression is essential for a subset of nasal glands, with other *Fgfs* compensating for the loss of *Fgf10* in some glands (May et al., 2016). The lateral nasal glands, for example, only require *Fgf10* for later gland branching stages, while the Steno's gland and the sinus glands require *Fgf10* expression earlier from gland initiation (May et al., 2016).

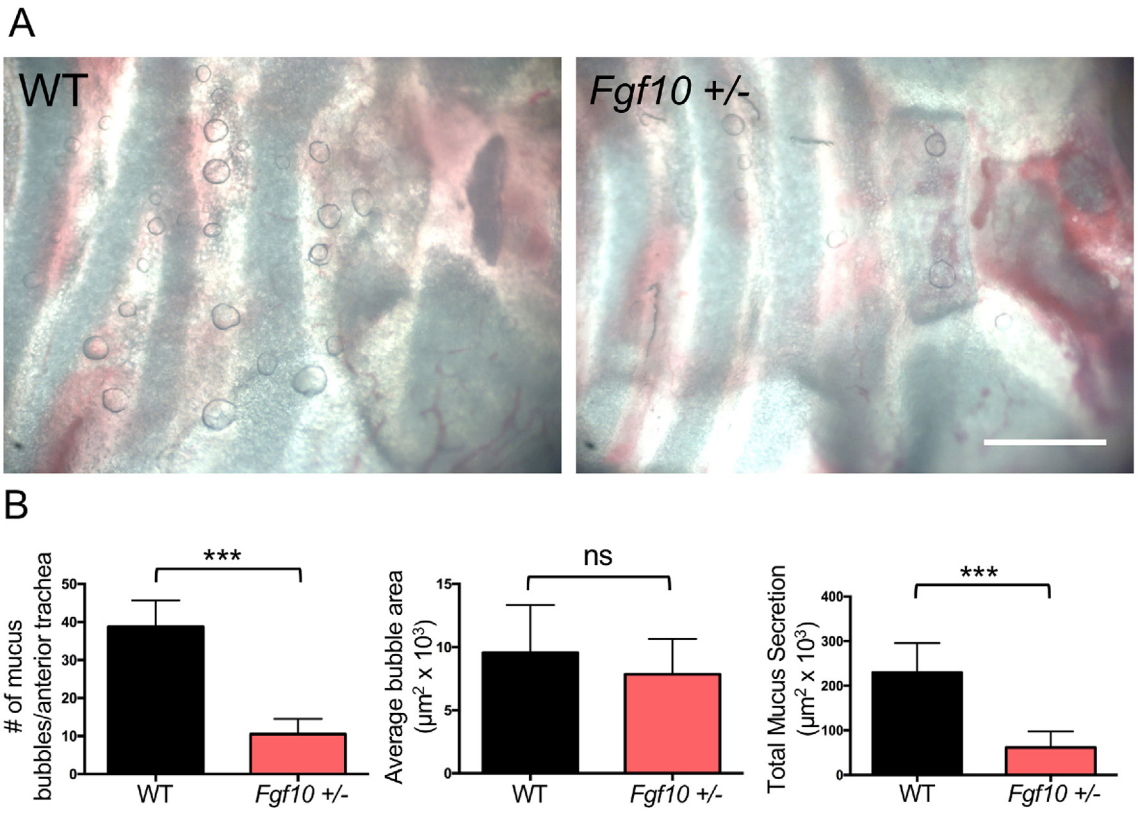

Fig. 4. *Fgf10* +/- adult mice have fewer tracheal SMGs and an overall reduction in mucus secretion. **(A)** Visualisation of functional gland openings in WT (n = 4) and *Fgf10* +/− (n = 6) anterior tracheal tissue by mucus bubble production. A decrease in the number of mucus bubbles was observed in *Fgf10* +/− mice. Scale bar = 500 μm. **(B)** Graphical representation of mucus bubble count, showing a significant reduction in number in *Fgf10*+/− animals compared to their WT littermates. Average bubble area was similar between the two groups, however overall mucus secretion into the airway lumen was significantly reduced in *Fgf10*+/− animals. *** = $p < 0.001$. Data in B are mean ± s.d.

The trachea SMGs therefore show a reliance on Fgf10 signalling more similar to the stenos and sinus glands.

As previously reported in other glands (May et al., 2016; Chatzeli et al., 2017), here we show that *Fgf10* is expressed in the mesenchyme adjacent to the gland epithelium during branching morphogenesis. Due to agenesis of the lungs *Fgf10* −/− mice die at birth (Sekine et al., 1999; Min et al., 1998), thereby preventing the study of later stages of tracheal gland development in the null mutant. Therefore, we adopted the use of a conditional *Fgf10* ablation model to investigate if tracheal SMGs could develop postnatally in the absence of FGF10 signalling. Ablation of *Fgf10* was induced at E17.5 and P2 and tracheal tissue was collected at P21. Histological analysis revealed a significant reduction in branching of the anterior glands adjacent to the cricoid cartilage in *CreERT2;Fgf10*$^{fl/fl}$ mice compared to wildtype littermates. Although minimal, some branching and cellular differentiation (indicated by mucus staining - blue) had occurred in the anterior gland epithelia. As our first tamoxifen administration may have taken 24 h to induce Cre-recombination, some residual Fgf10 may have promoted branching and mucus production in few SMG primordia that had initiated by E17.5/E18.5. Furthermore, as 100% Cre-recombination cannot be guaranteed, again some SMG placodes may have been exposed to low levels of Fgf10, inducing some cellular differentiation. To further assess the role of Fgf10 in cellular differentiation, analysis of differentiation markers such as AQP5 (Song et al., 2001) and MUC5b (Roy et al., 2014) would be required. In contrast, posterior SMGs, which develop postnatally, were reduced in *CreERT2;Fgf10*$^{fl/+}$ mice and completely absent in *CreERT2;Fgf10*$^{fl/fl}$ mice at P21, while the SMGs were found to have extended to C4 by this stage in WT littermates. This phenotype suggests one of two strategies: (1) bud outgrowth had occurred, however loss of *Fgf10* caused cell death in gland epithelium leading to no SMG buds evident by P21; or (2) Fgf10 is required for gland initiation and bud outgrowth in more posterior SMGs. In support of the latter, heterogeneous progenitor cell populations and signalling mechanisms are known to occur in the lung epithelium in an anterior/posterior axis. Cytokeratin-5 positive basal cells replenish the airway epithelium in the anterior trachea (Rock et al., 2009), while Clara cells are understood to be the main stem cell population of the more posterior tracheal epithelium (Rawlins et al., 2009). More recently, a study investigating airway epithelial regeneration following severe injury showed a multipotent SMG myoepithelial progenitor replenished airway epithelium in the anterior trachea (between CC-C1), with reduced replenishment observed in the posterior epithelium (C1-C4) (Lynch et al., 2018). Considering these heterogeneous mechanisms, while FGF10 may not be essential for anterior SMG bud initiation, it may be required for bud outgrowth in more posterior locations. This may also explain the phenotype observed in adult *Fgf10* +/- mice, where the posterior glands were more strongly affected. It is understood that mesenchymal Fgf10 regulates progenitor cell proliferation in adjacent branching epithelial structures in a number of different organs, such as the lung (Ramasamy et al., 2007), pancreas (Bhushan et al., 2001) and salivary gland (Chatzeli et al., 2017). For example, analysis of PCNA positive cells during lung development with reduced Fgf10 signalling revealed a significant decrease in proliferating cells in the lung epithelium, while proliferation was unchanged in the mesenchyme (Ramasamy et al., 2007). Further analysis of cell proliferation in both the anterior and posterior trachea will give insight into the role of Fgf10 in regulating this process in tracheal SMGs. The altered SMG phenotype in the conditionally ablated *Fgf10* model, and the global *Fgf10* heterozygous mouse is similar to the aplastic lacrimal and salivary gland phenotypes observed in patients that suffer from both ALSG and LADD syndrome (Milunsky et al., 2006; Shams et al., 2007; Entesarian et al., 2007). While no reports have stated any pulmonary defects in patients with ALSG or LADD syndrome, the airway SMGs may show aplasia and this phenotype could possibly give rise to muco-ciliary deficiencies in those that suffer from these autosomal dominant diseases. Furthermore, our functional tests of mucus secretion in *Fgf10* +/- adult mice conclude a significant reduction in total amount of mucus secreted into the airway lumen. As only the anterior glands were included in the study, an even greater difference would be assumed if all mucus bubbles extending posteriorly in WT animals had been calculated.

Previous reports have indicated that SMG development finishes by P21 in the mouse trachea (Rawlins and Hogan, 2005). However, in our analysis, WT mice only had SMGs extending down to the 4th tracheal cartilage ring (C4) at P21, in comparison to the 6–8 week WT mice where glands were observed at more posterior levels (Fig. 3, B). We therefore believe that posterior initiation of glands still occurs after 3 weeks. Later tamoxifen injection in the conditional mutants will allow us to study this further. In conclusion, we report that *Fgf10* expression in tracheal mesenchymal is essential for tracheal submucosal gland morphogenesis, in both late embryonic and early postnatal stages. Without this signalling factor, glands fail to develop, arresting at the bud stage anteriorly. Investigation into this developmental signalling cascade should be considered in further research attempting to understand the role of these organs in hyper-secretory respiratory diseases.

Acknowledgements

We would like to thank the Dental Institute of King's College London (Tucker, 2011) for funding May AJ. Teshima THN was funded by FAPESP (Fundação de Amparo à Pesquisa do Estado de São Paulo) (grant 2015/02824). Thanks to Mohammad Hajihosseini (University of East Anglia) for the Fgf10LacZ reporter mice. The Fgf10A02 tmc1c mice were obtained from the MRC-Harwell, which distributes these mice on behalf of the European Mouse Mutant Archive (http://www.emmanet.org). The MRC-Harwell is also a member of the International Mouse Phenotyping Consortium (IMPC), which funded the generation of the Fgf10A02 tmc1c mice. Associated primary phenotypic information may be found at http://www.mousephenotype.org.

Appendix A. Supplementary data

Supplementary data to this article can be found online at https://doi.org/10.1016/j.ydbio.2019.03.017.

References

Aikawa, T., et al., 1992. Marked goblet cell hyperplasia with mucus accumulation in the airways of patients who died of severe acute asthma attack. Chest 101 (4), 916–921.
Bhushan, a, et al., 2001. Fgf10 is essential for maintaining the proliferative capacity of epithelial progenitor cells during early pancreatic organogenesis. Development 128 (24), 5109–5117.
Borthwick, D.W., et al., 1999. Murine submucosal glands are clonally derived and show a cystic fibrosis gene-dependent distribution pattern. Am. J. Respir. Cell Mol. Biol. 20 (6), 1181–1189.
Bradley, A., et al., 2012. The mammalian gene function resource: the International Knockout Mouse Consortium. Mamm. Genome 23 (9–10), 580–586.
Buisine, M.P., et al., 1999. Developmental mucin gene expression in the human respiratory tract. Am. J. Respir. Cell Mol. Biol. 20 (2), 209–218.
Callea, M., et al., 2013. Ear nose throat manifestations in hypoidrotic ectodermal dysplasia. Int. J. Pediatr. Otorhinolaryngol. 77 (11), 1801–1804.
Chatzeli, L., Gaete, M., Tucker, A.S., 2017. Fgf10 and Sox9 are essential for the establishment of distal progenitor cells during mouse salivary gland development. Development 144 (12), 2294–2305.
Cho, H.-J., Joo, N.S., Wine, J.J., 2011. Defective fluid secretion from submucosal glands of nasal turbinates from CFTR-/- and CFTR (ΔF508/ΔF508) pigs. N. Vij PloS One 6 (8), e24424.
Danielian, P.S., et al., 1998. Modification of gene activity in mouse embryos in utero by a tamoxifen-inducible form of Cre recombinase. Curr. Biol. CB 8 (24), 1323–1326.
Entesarian, M., et al., 2007. FGF10 missense mutations in aplasia of lacrimal and salivary glands (ALSG). Eur. J. Hum. Genet. 15 (3), 379–382.
Finkbeiner, W.E., 1999. Physiology and pathology of tracheobronchial glands. Respir. Physiol. 118 (2–3), 77–83.
Hajihosseini, M.K., 2008. Fibroblast growth factor signalling in cranial suture development and pathogenesis. Front. Oral Biol. 12, 160–177.
Hannezo, E., et al., 2017. A unifying theory of branching morphogenesis. Cell 171 (1), 242–255 e27.
Hayashi, S., McMahon, A.J., 2002. Efficient recombination in diverse tissues by a tamoxifen-inducible form of cre: a tool for temporally regulated gene activation/inactivation in the mouse. Dev. Biol. 244, 305–318.
Hoegger, M.J., et al., 2014. Impaired mucus detachment disrupts mucociliary transport in a piglet model of cystic fibrosis. Science 345 (6198), 818–822.

Ianowski, J.P., et al., 2007. Mucus secretion by single tracheal submucosal glands from normal and cystic fibrosis transmembrane conductance regulator knockout mice. J. Physiol. 580 (Pt 1), 301–314.
Jaskoll, T., et al., 2005. FGF10/FGFR2b signaling plays essential roles during in vivo embryonic submandibular salivary gland morphogenesis. BMC Dev. Biol. 5, 11.
Jeong, J.H., et al., 2015. Secretion rates of human nasal submucosal glands from patients with chronic rhinosinusitis or cystic fibrosis. Am. J. Rhinol. Allergy 29 (5), 334–338.
Joo, N.S., et al., 2001. Optical method for quantifying rates of mucus secretion from single submucosal glands. Am. J. Physiol. Lung Cell Mol. Physiol. 281 (2), L458–L468.
Joo, N.S., et al., 2010. Hyposecretion of fluid from tracheal submucosal glands of CFTR-deficient pigs. J. Clin. Investig. 120 (9), 3161–3166.
Kelly, R.G., et al., 2001. The arterial pole of the mouse heart forms from Fgf10-expressing cells in pharyngeal mesoderm. Dev. Cell 1, 435–440.
Keswani, S.G., et al., 2011. Submucosal gland development in the human fetal trachea xenograft model: implications for fetal gene therapy. J. Pediatr. Surg. 46 (1), 33–38.
Klockars, M., Reitamo, S., 1975. Tissue distribution of lysozyme in man. J. Histochem. Cytochem. 23 (12), 932–940.
Lizen, B., et al., 2015. Perinatal induction of Cre recombination with tamoxifen. Transgenic Res. 24, 1065–1077.
Lynch, T.J., et al., 2018. Submucosal gland myoepithelial cells are reserve stem cells that can regenerate mouse tracheal epithelium. Cell Stem Cell 22 (5), 653–667.
Mailleux, A.A., et al., 2002. Role of FGF10/FGFR2b signaling during mammary gland development in the mouse embryo. Development 129, 53–60.
Makarenkova, H.P., et al., 2000. FGF10 is an inducer and PAX6 a competence factor for lacrimal gland development. Development 127, pp2563–2572.
Masson, P.L., et al., 1966. Immunohistochemical localization and bacteriostatic properties of an iron-binding protein from bronchial mucus. Thorax 21 (6), 538–544.
May, A., Tucker, A., 2015. Understanding the development of the respiratory glands. Dev. Dynam. 244 (4), 525–539.
May, A.J., et al., 2016. FGF and EDA pathways control initiation and branching of distinct subsets of developing nasal glands. Dev. Biol. 419 (2), 348–356.
May, A.J., et al., 2015. Salivary gland dysplasia in Fgf10 heterozygous mice: A new mouse model of xerostomia. Curr. Mol. Med. 1–9.
Milunsky, J.M., et al., 2006. LADD syndrome is caused by FGF10 mutations. Clin. Genet. 69 (4), 349–354.
Min, H., et al., 1998. Fgf-10 is required for both limb and lung development and exhibits striking functional similarity to Drosophila branchless. Genes Dev. 12 (20), 3156–3161.
De Moerlooze, L., et al., 2000. An important role for the IIIb isoform of fibroblast growth factor receptor 2 (FGFR2) in mesenchymal-epithelial signalling during mouse organogenesis. Development 127 (3), 483–492.
Ohuchi, H., Hori, Y., Yamasaki, M., Harada, H., Sekine, K., et al., 2000. FGF10 acts as a major ligand for FGF receptor 2 IIIb in mouse multi-organ development. Biochem. Biophys. Res. Commun. 277, 643–649.
Oppenheimer, E., Esterly, J., 1975. Pathology of cystic fibrosis: review of the literature and comparison with 146 autopsied cases. In: Rosenberg, H., Bolande, R. (Eds.), Perspectives in Pediatric Pathology. Yearbook Medical Publishers, Chicago, USA, pp. 241–278.
Ornitz, D., Itoh, N., 2001. Fibroblast growth factors. Genome Biol. 2 (3), 1–12.
Ramasamy, S.K., et al., 2007. Fgf10 dosage is critical for the amplification of epithelial cell progenitors and for the formation of multiple mesenchymal lineages during lung development. Dev. Biol. 307 (2), 237–247.
Rawlins, E., et al., 2009. The role of Scgb1a1+ Clara cells in the long-term maintenance and repair of lung airway, but not alveolar, epithelium. Cell Stem Cell 4 (6), 525–534.
Rawlins, E.L., Hogan, B.L.M., 2005. Intercellular growth factor signaling and the development of mouse tracheal submucosal glands. Dev. Dynam. 233 (4), 1378–1385.
Reid, L., 1960. Measurement of the bronchial mucous gland layer: a diagnostic yardstick in chronic bronchitis. Thorax 15, 132–141.
Rice, R., Spencer-Dene, B., Connor, E.C., Gritli-Linde, A., McMahon, A.P., et al., 2004. Disruption of Fgf10/Fgfr2b-coordinated epithelial-mesenchymal interactions causes cleft palate. J. Clin. Invest. 113, 1692–1700.
Rock, J.R., et al., 2009. Basal cells as stem cells of the mouse trachea and human airway epithelium. Proc. Natl. Acad. Sci. U. S. A. 106 (31), 12771–12775.
Rogers, D.F., 2004. Airway mucus hypersecretion in asthma: an undervalued pathology? Curr. Opin. Pharmacol. 4 (3), 241–250.
Rogers, D.F., 2008. Airway mucus hypersecretion in asthma and COPD: not the same? In: Barnes, P., et al. (Eds.), Asthma and COPD. Basic Mechanisms and Clinical Management. Academic Press Inc., pp. 211–223
Roy, M.G., et al., 2014. Muc5b is required for airway defense. Nature 505, pp412–416.
Sala, F.G., et al., 2011. FGF10 controls the patterning of the tracheal cartilage rings via Shh. Development 138, 273–282.
Salinas, D., et al., 2005. Submucosal gland dysfunction as a primary defect in cystic fibrosis. FASEB J. Off. Publ. Fed. Am. Soc. Exp. Biol. 19 (3), 431–433.
Sekine, K., et al., 1999. Fgf10 is essential for limb and lung formation. Nat. Genet. 21 (1), 138–141.
Shams, I., et al., 2007. Lacrimo-auriculo-dento-digital syndrome is caused by reduced activity of the fibroblast growth factor 10 (FGF10)-FGF receptor 2 signaling pathway. Mol. Cell Biol. 27 (19), 6903–6912.
Skarnes, W.C., et al., 2011. A conditional knockout resource for the genome-wide study of mouse gene function. Nature 474 (7351), 337–344.
Steinberg, Z., et al., 2005. FGFR2b signaling regulates ex vivo submandibular gland epithelial cell proliferation and branching morphogenesis. Development 132, 1223–1234.
Sturgess, J., Imrie, J., 1982. Quantitative evaluation of the development of tracheal submucosal glands in infants with cystic fibrosis and control infants. Am. J. Pathol. 106 (3), 303–311.
Song, Y., et al., 2001. Role of aquaporin water channels in airway fluid transport, humidification , and surface liquid hydration. J. Gen. Physiol. 17, 573–582.
Teshima, T.H.N., Lourenço, S.V., Tucker, A.S., 2016. Multiple cranial organ defects after conditionally knocking out Fgf10 in the neural crest. Front. Physiol. 7, 488.
Thurlbeck, W., Benjamin, B., Reid, L., 1961. Development and distribution of the mucous glands in the foetal human trachea. Br. J. Dis. Chest 55, 54–64.
Tucker, A.S., 2007. Salivary gland development. Sem. Cell Dev. Biol. 18, 237–244.
Wells, K.L., et al., 2013. Dynamic relationship of the epithelium and mesenchyme during salivary gland initiation: the role of Fgf10. Biol. Open 2 (10), 981–989.
Xie, W., et al., 2014. Sox2 modulates Lef-1 expression during airway submucosal gland development. Aust. J. Pharm. Lung Cell. Mol. Physiol. 306 (7), L645–L660.